

Questions on pure luminosity evolution for ellipticals

Ping He², and Yuan-Zhong Zhang^{1,2}

¹ *CCAST (World Laboratory), P.O.Box 8730, Beijing 100080, P.R. China (yzhang@itp.ac.cn)*

² *Institute of Theoretical Physics, Academia Sinica, P.O.Box 2735, Beijing 100080, P.R. China (hemm@itp.ac.cn)*

ABSTRACT

The explanation for the existence of an excess population of faint blue galaxies (FBGs) has been a mystery for nearly two decades, and remains one of the grand astronomical issues to date. Existing models cannot explain all of the observational data such as galaxy number counts in the optical and infrared passbands and the redshift distributions of galaxies. Here, by modelling the morphological number counts derived from the Hubble Space Telescope, as well as the number counts in optical and infrared passbands, and the redshift and color distributions of galaxies obtained from ground-based observations, we show that the ‘FBG problem’ cannot be resolved if elliptical galaxies are assumed to have formed in an instantaneous burst of star formation at high redshift with no subsequent star formation events, which is just the conventional scenario for formation and evolution of ellipticals. There exist great discrepancies between the observed $B - K$ color distribution and the predicted distribution for ellipticals by such a pure luminosity evolution (PLE) model in the context of the conventional scenario. Neither can the mild evolution (i.e., the star formation events have lasted for a longer time than those of the instantaneous burst and passive evolution since the formation of galaxies) for ellipticals be accepted in the context of PLE assumption. The introduction of dust extinction also cannot save the PLE models. This conclusion holds for each of the three cosmological models under consideration: flat, open and Λ -dominated. Hence, our investigation suggests that PLE assumption for elliptical galaxies is questionable, and number evolution may be essential for ellipticals.

Subject headings: cosmology: miscellaneous – galaxies: elliptical and lenticular, cD – galaxies: evolution – galaxies: luminosity function, mass function – galaxies: statistics

1. Introduction

The number counts of galaxies at deep blue (B , $\lambda_{eff}=4500 \text{ \AA}$) and near-infrared (K , $\lambda_{eff}=2.2 \text{ \mu m}$) wavelengths produce conflicting results: the B -band counts show an excess over the no-evolution predictions, and suggest strong luminosity evolution in galaxy populations, while the K -band counts are well fit by the non-evolutionary models. When spectroscopic samples became available, it was found that the redshift distributions of galaxies were also consistent with the non-evolutionary predictions and strong luminosity evolution would lead to a high- z distribution, overestimating the observations. This is the common statement of the problem of the excess population of faint blue galaxies (FBGs), which remains one of the grand astronomical issues (Koo & Kron 1992; Ellis 1997). To get out of these paradoxes, a number of scenarios have been suggested, including: (1) pure luminosity evolution in galaxy populations, which increases the distance to which galaxies may be seen (Tinsley 1980; Bruzual & Kron 1980; Koo 1981, 1985; Guiderdoni & Rocca-Volmerange 1990; Gronwall & Koo 1995; Pozzetti, Bruzual, & Zamorani 1996); (2) the choice of a cosmological geometry that maximizes the available volume, either by adoption of a low value of the deceleration parameter q_0 (an open cosmological model) or by introducing a cosmological constant λ_0 (Broadhurst, Ellis & Shanks 1988; Colless et al. 1990; Cowie, Songaila & Hu 1991; Colless et al. 1993; Fukugita et al. 1990); or (3) increasing the number of galaxies at earlier times, either by introducing additional populations, which once existed at high z but have since disappeared or self-destructed (Broadhurst, Ellis, & Shanks 1988; Cowie 1991; Babul & Rees 1992; Babul & Ferguson 1996), or by merging, that is by assuming that present-day galaxies were in smaller fragments at high redshifts (Rocca-Volmerange & Guiderdoni 1990; Cowie et al. 1991; Guiderdoni & Rocca-Volmerange 1991; Broadhurst, Ellis & Glazebrook 1992; Carlberg & Charlot 1992; Kauffmann, Guiderdoni & White 1994; Roukema et al. 1997). There are still many uncertainties in the FBG problem, and we are in need of more inputs, especially from observations, in order to constrain the models.

Great progress has been made recently in observational cosmology through the use of Hubble Space Telescope (HST), whose unprecedented imaging ability enables galaxies to be segregated morphologically into several wide classes (Glazebrook et al. 1995a; Driver et al. 1995; Abraham et al. 1996). With morphological data it becomes possible to simplify the modelling of FBGs so that each morphological type can be modelled independently, thereby reducing the complexity of each individual model (Driver & Windhorst 1995).

Following this line of thought, in a previous investigation (He & Zhang 1998a, hereafter HZ98) we have modelled the number counts of E/S0 galaxies obtained from the Medium Deep Survey (MDS) and the Hubble Deep

Field (HDF) in the HST I_{814} -bandpass ($\lambda_{eff}=8000 \text{ \AA}$), and found that the number counts of ellipticals could be well explained by PLE models in any cosmological geometry under consideration if ellipticals are assumed to have formed at high redshift (say $z_f=5.0$) and thereafter have passively evolved (i.e., no further star formation). This is just the traditional scenario for the formation and evolution of elliptical galaxies (Eggen, Lynden-bell, & Sandage 1962; Partridge & Peebles 1967). The models with a larger timescale of star formation rate (SFR) which takes the exponential decay form cannot reproduce well the number counts, while the models with z_f as low as, say $z_f=2.5$, in an open or Λ -dominated universe produce a dramatically high tail or high peak in redshift distributions, though they predict the number counts fairly well. In particular, we emphasize that the cosmological geometry can not be constrained by such number counts for ellipticals, in disagreement with the conclusion of Driver et al. (1996), who concluded that flat models dominated by a cosmological constant are ruled out from comparison of their E/S0 number counts (Driver et al. 1995) with their model predictions. The reader is referred to HZ98 for details.

But such a scenario for ellipticals needs to be verified further by modelling other Hubble types (i.e., early- and late-type spirals and irregulars as separated by HST) and the overall population of galaxies, and should be constrained by other observational data such as redshift distributions and color distributions obtained from ground-based telescopes.

Incorporating other observations and modelling of the other types, we now find that the FBG problem cannot be resolved by the conventional scenario for elliptical galaxy formation. Though such PLE models can roughly reproduce the galaxy number counts in the blue and infrared passbands as well as the magnitude limited redshift distribution, there exist great discrepancies between the observed $B - K$ color distribution and the predicted distribution for ellipticals by such a conventional scenario. The inclusion of mild luminosity evolution and dust extinction also cannot save the scenario. This conclusion holds in each of the three cosmological models under consideration: flat, open and Λ -dominated. Our investigation suggests that number evolution may be essential for ellipticals.

Number evolution models have been widely considered to account for the paradoxes concerning the FBG problem. One of the considerations on number evolution is merging between galaxies, which is a natural feature of hierarchal theory for the growth of structure by gravity. Notice that a new type of models, i.e., semi-analytic models have appeared recently (Cole 1991; White & Frenk 1991; Lacey et al. 1993; Kauffmann, White & Guiderdoni 1993; Kauffmann et al. 1994; Cole et al. 1994; Baugh, Cole & Frenk 1996), which are well physically motivated by cosmological theory, and may eventually provide the greatest understanding of galaxy formation and evolution (Gardner

1998). The traditional galaxy number count models (e.g., Yoshii & Takahara 1988; Guiderdoni & Rocca-Volmerange 1990; Gardner 1998), however, are still powerful tools to explore the formation and evolutionary history of galaxies, and can be treated as complements to the semi-analytic techniques. We will make use of the traditional approach throughout this work.

Finally, we construct a set of simple number-luminosity evolution (NLE) models to explain the number counts and color-selected redshift distributions in the B -band for elliptical galaxies. We argue that the number evolution is necessary for reconciling the conflicts above-mentioned. In particular, if the cosmic geometry is open or Λ -dominated, our work supports the idea that ellipticals formed by mergers of spiral galaxies, which is compatible with the prediction of hierarchical theory for formation and evolution of galaxies.

In section 2 we briefly review the procedure for the construction of the models. The results of the models are shown in Section 3 for comparison with the observational data, and a phenomenological number evolution model is presented in Section 4. We will give the summary and conclusions in Section 5.

2. Construction of models

We employ the latest version of the galactic spectral synthesis models of Bruzual & Charlot (1997), with solar metallicity, to compute the evolutionary spectral energy distributions (SEDs) for the galaxies. In the BC code, model galaxies are characterized by the initial mass function (IMF) and the SFR. Throughout this work, we assume the standard Salpeter IMF (1955) for the other Hubble types than early-type galaxies, while a Scalo IMF (1986) for ellipticals. The Scalo IMF is more suitable for ellipticals than the Salpeter IMF in that a less steep IMF at the high-mass end such as the Salpeter one will lead to more massive stars existing at early times, rendering UV fluxes are so strong that more galaxies can be detected at high z , and hence, even with dust extinction involved, the models will overpredict the number counts for ellipticals between $I_{814} \sim 19$ and 21 (cf. HZ98). The SFR, $\psi(t)$, is chosen as an exponential decay form with respect to time t , i.e., $\psi(t) \sim \exp(-t/\tau_e)$, where τ_e , measured in Gyr, is the timescale characterizing this form of the SFR. τ_e is treated as a free parameter to be adjusted to reproduce the local photometric and spectroscopic properties, such as present-day colors and spectra for galaxies. For comparison, we list the local observed colors of galaxies in Table 1. We have also considered to some extent the effect of dust extinction, following Wang's (1991) prescription and similar to that of HZ98. The extinction magnitudes in the B , I , and K passbands for galaxies of a typical luminosity L^* are listed in Table 2. By adopting both the Scalo IMF (for ellipticals) and the dust extinction, the UV flux at early times can be greatly reduced so as to avoid the detection of a large

number of galaxies at high- z , which are not observed in current deep surveys.

Predictions for the color distribution of galaxies in a given range of apparent magnitude $[m_{\lambda 1}, m_{\lambda 2}]$ can be computed by integrating the following equation over m_λ and z ($z \leq z_{max}$), as:

$$N(c) = \int_{c < c(z) < c+dc} \int_{m_{\lambda 1}}^{m_{\lambda 2}} d^2 N(m_\lambda, z) dm_\lambda dz, \quad (1)$$

where $z_{max} = \min(z_f, z_L)$, with z_f being the formation redshift for galaxies, and z_L being the redshift above which the Lyman continuum break enters the λ -filter. $c(z)$ is the color-redshift relation for galaxies. In order to compute the differential color distribution $dN(c)$, which is a function of color c , the integration over z is restricted by the inequality $c < c(z) < c+dc$, such as the color $c(z)$ is in the relevant color bin dc in the color range $[c, c+dc]$. In the above integral, $d^2 N(m_\lambda, z)$ refers to the differential number counts for galaxies in the intervals $[m_\lambda, m_\lambda+dm_\lambda]$ and $[z, z+dz]$. Its explicit expression, as well as the formulae which we need in this work to compute the number counts and redshift distributions, can be found in, e.g., Guiderdoni & Rocca-Volmerange (1990) or HZ98. To make the predictions more realistic, we smooth the differential color distribution $dN(c)$ in the colour interval $c \sim c+dc$ by a Gaussian profile with $\sigma = 0.20$ mag before deriving the integrated distribution, which is slightly different from the prescription of Pozzetti et al. (1996), while similar to that of Gardner (1998). This procedure is expected to mimic the observational errors in the colours as well as the intrinsic dispersion in the colours of galaxies of the same Hubble type.

Following the prescription of HZ98, we adopt three representative cosmological models in this work: 1) flat, $\Omega_0 = 1.0$, $\lambda_0 = 0$, and $h = 0.5$ ($H_0=100 h \text{ km s}^{-1} \text{ Mpc}^{-1}$) (hereafter, Scenario A); 2) open, $\Omega_0 = 0.1$, $\lambda_0 = 0$, and $h = 0.5$ (Scenario B); and 3) flat and Λ -dominated, $\Omega_0 = 0.2$, $\lambda_0 = 0.8$, and $h = 0.6$ (Scenario C). We assume a formation redshift $z_f = 5.0$ for all types of galaxies in all three cosmological models.

3. Results

3.1. Luminosity functions

The luminosity functions (LFs) of galaxies, which is the distribution law of the number density of galaxies against their absolute luminosities, is an important ingredient for modelling. However, the LFs for present-day galaxy populations are not well-determined by local surveys, and the universality of LFs are doubtful. Hence we treat the parameters of LFs as free to be adjusted to give the best fit of the morphological number counts. The LFs take the Schechter form (Schechter 1976) for present-day galaxies, and we list the parameters (α , ϕ^* , and M_B^*) of these (B -

band) LFs in Table 3. LFs in other pass-bands can be obtained by shifting corresponding present-day colors. The model LFs are also shown in Figure 1 to compare with the observed ones. It can be seen from Figure 1 that, in both the B - and the K -bands, the faint-end slopes of model LFs are steeper than those of the observed ones whatever the cosmological models will be. The reason for such adoptions will be given in Section 3.3.1.

Besides, the PLE models alone cannot reproduce the steep slope of the number counts at faint magnitudes in the I_{814} -band for late-type spirals/irregulars in a flat cosmological model (Scenario A), so we enhance the characteristic number density ϕ^* of the LF for the Sdm galaxies with respect to look-back time δt as $\phi^*(\delta t) = \phi_0^*(\beta \frac{\delta t}{t_0})$ ($\beta > 0$), where the subscript ‘0’ refers to present-day values.

3.2. Star formation rates

The parameter τ_e of the SFR for galaxies is adjusted to reproduce the local photometric and spectroscopic properties of galaxies, such as local colors and spectra (cf. Fukugita, Shimasaku, & Ikhikawa 1995; Yoshii & Takahara 1988). We summarize the values for this parameter for all the Hubble types in column 2 of Table 3. In particular, the case of $\tau_e = 0$ for ellipticals (Scenario B) represents *purely* passive evolution and a constant SFR for the Sdm galaxies is denoted by $\tau_e = \infty$. It can be seen from Table 3 that the modelled colors are close to the corresponding observed ones (see Table 1). Considering that there are uncertainties of 0.1 – 0.2mag in colors, the values of τ_e of our models are acceptable.

In the following, we will examine whether the models based on these LF and SFR parameters can be accepted by comparing the modelled galaxy number counts, redshift and color distributions with those observed.

3.3. Number counts

3.3.1. Morphological number counts

Corresponding to the morphological classification of galaxies by HST, we incorporate Sab and Sbc galaxies into early-type spirals, and Scd and Sdm galaxies into late-type spirals/irregulars. With $\beta = 1.5$ for Scenario A (see above for the reason of the introduction of β), we can see from Figure 2 that the models can reproduce well the number counts in the I_{814} -band for all three galaxy types as well as for the overall population in any cosmological model under consideration. We see that, in order to reproduce the number counts for early-type spirals and late-type spirals/irregulars at faint magnitudes with the least additional assumptions other than PLE, it is necessary to adopt steep faint-end slopes of LFs for those galaxy populations.

3.3.2. Number counts in blue and near-infrared bands

From Figure 3 we can see that the models can reproduce better the number counts only at bright magnitudes in both the B ($B < 21$) and the K ($K < 17$) bands, indicating that the normalization (involving both ϕ_0^* and L^* , cf. Ellis 1997) is proper by the adoptions of LFs¹. The discrepancies between the model predictions and the observations exist at the faintest magnitudes in both B - and K - bands. It seems that there are not sufficient blue galaxies to reproduce the steep slope at the faintest magnitudes in the B -band, whereas in the K -band, it seems that too many red galaxies are predicted over the observations. These red objects are ellipticals, which dominate at most of the K magnitudes in contrast with the case in the B -band. However, given the uncertainties in faint galaxy number counts due to either small sample sizes or galaxy clustering, we can still consider the PLE predictions to be in rough agreement with the observations, but we should emphasize that the agreement is achieved by the adoption of steep slopes for LFs of late-type galaxies. If the slopes are as low as $\alpha \sim -1$, the discrepancies are expected to be large, especially for the flat Einstein-de Sitter universe (Scenario A).

3.4. Redshift distribution for $K < 20$

The spectroscopic studies with the LRIS spectrograph on the Keck Telescope of two of the Hawaii deep survey fields SSA 13 and SSA 22 (Cowie et al. 1996) present one of the largest and deepest redshift samples, and provide a powerful tool for understanding the evolution of galaxies. Compared with optical light, the absolute K -band magnitude is mostly contributed to by near-solar-mass stars in which make up the bulk of galaxies. It is therefore a good tracer of the baryonic mass and particularly suitable for the study of old stellar populations. Furthermore, the SEDs at low redshifts at near-infrared wavelengths for different morphological classes of galaxies are very similar, and hence the morphological mix will be insensitive to redshift if there is no evolution, and any evolutionary signature will be more clearly seen (Glazebrook 1997).

From the Cowie et al. (1996) sample, we have derived the redshift distribution limited at $K < 20$, with the total number being 207, and the completeness being 100% for $K < 18$ and 72% for $18 < K < 20$. We compare predictions of our models with the observed data in Figure 4. It can be seen that our models predict more high- z objects than the observation in the three Scenarios, and most of them are ellipticals. However, given that the redshift data for $K > 18$ is only 72% complete, one might suppose that much of the high- z discrepancy here is due to incomplete-

¹Due to large uncertainties in determining the present-day LFs, the normalization of LFs is usually chosen to scale the model predictions to the observed number counts at a fainter magnitude, say $B \sim 19.0$, rather than at the brightest end, see Pozzetti et al. 1996 for a comprehensive review about this.

ness (see the comment on the incompleteness by Pozzetti et al. 1996), we argue that the PLE models cannot be ruled out from comparison with the observed data.

3.5. $B - K$ color distribution for $17 < K < 20$

Since the redshift distribution from the Cowie et al. (1996) sample is complete to only $\sim 70\%$ for fainter magnitudes in $18 < K < 20$, the failure existing in the PLE models can be exposed by using the $B - K$ color distribution for galaxies from $17 < K < 20$ in the same Hawaii sample, whose completeness in the $B - K$ color statistics limited in $17 < K < 20$ is 100%. From Figure 5, we see that none of the models can satisfactorily reproduce the observations. In any case, the colors of early- and late-type spirals and irregulars will not be redder than $B - K \sim 5.5$ according to our spectrophotometric models, and ellipticals should be responsible for the objects at the red-end of the distribution. But the models underpredict the data between $B - K = 5.0 - 8.0$ and produce extremely red humps beyond $B - K = 8.0$. The great discrepancies between the observations and the model predictions indicate that the models need substantial revising. It should be pointed out that the predicted color distributions are not sensitive to the specific adoptions of LFs, but sensitive to the star formation rate of galaxies.

It can be seen that the $B - K$ color distribution for galaxies can efficiently reveal the defects of the PLE models based on the assumption of *purely* passive evolution of ellipticals.

3.6. Mild evolution in luminosity for ellipticals

From the above analysis of the $B - K$ color distribution for galaxies, we find that far more extremely red ($B - K > 8$) ellipticals than observed are predicted by our PLE models in the context of the traditional scenario for formation and evolution of ellipticals, and these models are not acceptable. For the sake of comparison, we reconsider the modelling for ellipticals with the assumption of mild luminosity evolution. *Mild evolution* here means that the star formation events have lasted for a longer time than those of the instantaneous burst and passive evolution since the formation of galaxies. Explicitly speaking, the SFR timescale τ_e for mild evolution should be slightly larger than that for passive evolution. By assuming $\tau_e = 1.0$ Gyr (the modelled $B - K$ colors are 4.07, 4.18, and 4.18 for Scenario A, B, and C, respectively), we can see from Figure 6a that such PLE models as mild luminosity evolution overpredict the number counts at faint magnitudes in the I_{814} -band for Scenarios B and C, and hence these mild evolution models are also not acceptable. However, the model prediction for Scenario A appears to fit the data reasonably well.

From the previous analysis of color distribution in Section 3.5, we have found that ellipticals can be discriminated from the other Hubble types by $B - K$ color, so that no

objects except ellipticals can be redder than $B - K = 5.5$. It is worthwhile mentioning that the significance of color-selected sub-sample for investigating the evolution of ellipticals has been first realized by Kauffmann, Charlot, & White (1996), but their scheme of selecting ellipticals by means of color is slightly different from ours, in which we pick out ellipticals by $B - K$ color solely rather than the color-redshift relation. Applying this color-selection criterion to the current case, we derive from the Cowie et al. (1996) sample the redshift distribution for galaxies limited to $22.5 < b_j < 24.0$ and subject to the condition $B - K > 5.5$. It can be seen from Figure 6b that observationally, ellipticals are completely absent at high- z beyond $z = 0.8$, consistent with a recent report by Zepf (1997) from the analysis of deep optical and infrared images derived from HST. However, our Scenario A model underpredicts the objects in the intermediate redshift interval ($0.3 < z < 0.8$), and overpredicts the high- z distribution, extending to redshifts as high as 1.4, completely in disagreement with the observations. Hence, we arrive at the conclusion that the PLE models with mild evolution cannot be accepted either in any cosmological model under consideration.

4. Number-luminosity evolution for ellipticals

As demonstrated above, PLE models solely are not the appropriate simulations for formation and evolution of ellipticals. In any realistic evolutionary models for galaxies, however, luminosity evolution must be considered due to the aging of stellar populations, which leads to the continuous change of photometric and spectroscopic properties of galaxies. For simplicity, however, we use the same galaxy evolution models with mild luminosity evolution as in the above PLE models (Section 3.6) to compute the K - and e -corrections for galaxies, without considering more complicated star formation scenarios (e.g., Colín, Schramm, & Peimbert 1994; Fritze-v. Alvensleben & Gerhard 1994), or various complicated physical processes concerning the formation of galaxies (cf. Roukema et al. 1997).

Without considering the underlying physical mechanism, we phenomenologically formulate the number evolution for ellipticals by the expression $\phi^*(z) = \phi_0^* f_\phi(z)$, where $f_\phi(z)$ represents the following function:

$$f_\phi(z) = \begin{cases} (1+z)^{-Q_{n1}}, & z \leq z_t; \\ (1+z_t)^{-Q_{n1}} \left(\frac{z-z_f}{z_t-z_f}\right)^{Q_{n2}}, & z_t < z \leq z_f, \end{cases} \quad (2)$$

and for consistency, we assume the characteristic mass M^* of mass function (MF) for galaxies decreasing with respect to redshift z as $M^*(z) = M_0^* f_M(z)$, where $f_M(z)$ represents the following function:

$$f_M(z) = (1+z)^{-Q_m}, \quad (3)$$

and for simplicity, we assume the faint-end slope α of LF does not change with z , and the evolution of LF maintains

the property of self-similarity. Hence the number evolution model is characterized by the parameters Q_{n1} , Q_{n2} , Q_m and the redshift z_t . The MF can be translated into LF by the present-day mass/luminosity ratio of galaxies, and the evolution of LF exactly follows the same formulae as Eq. [2] and [3]. We expect such a simple treatment can to the most extent reflect the basic features of the evolutionary history for ellipticals without getting bogged down into too many technical details. Our NLE model presented here, if $z_t = z_f$, is similar to the $M^*-\phi^*$ model designed by Guiderdoni & Rocca-Volmerange (1991). Obviously, the NLE model degenerates to PLE model when $z_t = z_f$ and $Q_{n1} = Q_m = 0$.

We have tentatively determined a set of these parameters (z_t , Q_{n1} , Q_{n2} , and Q_m) by trial and error, whose values are listed in Table 4. We show the predictions of the NLE models and compare with the observed number counts for ellipticals in Figure 7a. We see that, in contrast with the predictions of PLE models with mild luminosity evolution presented in Section 3.6, the predictions of the NLE models are satisfactory; in particular, they can reproduce well the faint-end counts as well as the flattening in any world model under consideration. We have also presented in Figure 7b the predictions of the z -distributions to compare with the same color-selected sample as in Section 3.6. It can be seen that our model predictions are in gross agreement with the color-selected sample for Scenario B and C, and do not show significant high- z tails. The NLE prediction for Scenario A is better than the case of PLE, but it still overestimates the high- z distributions. This discrepancy between the model prediction and observed data should be regarded not as the rejection of the flat cosmological model ($\Omega_0 = 1$) but, we believe, as the indication that the model needs further elaborating, since we have not considered, for example, the evolution of metallicity with respect to z , and the $(1+z)^4$ dependence of the surface brightness with respect to z for the sake of simplicity (cf. Yoshii & Peterson 1995). As addressed by Pozzetti et al. (1996), the magnitude of this effect not only is a function of various intrinsic parameters of galaxies, but also depends on the data reduction procedure. This effect, if considered in our models, could be expected to further reduce the number of ellipticals at high z .

In Figure 8 we show the predicted $B-K$ color distributions with the mild luminosity evolution and the number evolution which follows the expression of Eq. [2] and [3]. It seems that the NLE models do not reproduce satisfactorily the $B-K$ color distribution, but we can see that the red-end humps have disappeared, which to some extent indicates the success of the models. As for the discrepancies between the predictions and the observation, we argue that they might reflect that the spectrophotometric models need further elaborating, e.g. fine-tuning the SFR timescale τ_e for ellipticals or dividing ellipticals into several sub-classes with different τ_e specified for each of them. We

will consider these possibilities elsewhere (cf. He & Zhang, 1998b).

5. Summary and Conclusions

The assumption of pure luminosity evolution is no doubt the starting point for investigating the formation and evolution of galaxies. Traditionally, ellipticals are believed to evolve passively after they formed in an instantaneous burst of star formation, and indeed the models based on such an assumption can reproduce fairly well the number counts for ellipticals (HZ98), but in this work we find that such PLE models completely fail to account for the $B-K$ color distribution limited in the faint K magnitude bin of $17 < K < 20$. On the other hand, the models with mild luminosity evolution in the context of PLE assumption will overestimate the faint-end elliptical number counts in an open or Λ -dominated cosmological models (Scenario B and C), or overpredict the high- z objects in the flat universe (Scenario A), significantly in disagreement with the color-selected redshift distribution (see Figure 6), and hence also cannot be accepted. It seems that the PLE models for ellipticals, whether the luminosity evolution is purely passive, as assumed by traditional scenario, or mild, cannot reconcile simultaneously the number counts and color distribution for ellipticals. Therefore, these paradoxes indicate that the evolution within the population of elliptical galaxies may be more complicated than that expected by the PLE assumption.

These conflicts exist in all three cosmological models considered here, indicating that changing cosmological geometry is not a ‘graceful exit’. Furthermore, dust extinctions will both shift the red-end humps even redder and decrease the number of ellipticals in the $B-K$ color distribution, and hence also cannot save the traditional scenario for ellipticals. We are obliged to abandon the pure luminosity evolution scenario for ellipticals when facing these conflicts.

We have not restricted ourselves to any ‘observed’ LFs due to the various uncertainties in determining them locally. Models based on such ‘observed’ LFs can not even reproduce the morphological number counts. Instead, we treat the LF parameters α , ϕ^* , and M^* as free parameters to be adjusted to reproduce the morphological number counts. Most importantly, our results, e.g., the predicted $B-K$ color distributions, do not critically depend on specific adoptions of LFs. Our conclusions are robust unless the observational data are plagued with great uncertainties or biases, such as errors in morphological classification for galaxies, selection effects, or even unrealized systematic errors.

If the assumption of PLE has to be abandoned, then number evolution for ellipticals should be a rational inference. As mentioned in Introduction, an additional galaxy population is usually considered as a plausible proposal to account for the excess faint galaxies observed at opti-

cal bands, which once existed at early epochs but disappeared or self-destructed subsequently, and hence cannot be detected by local surveys. However, if such an additional population were introduced into the modelling, in principle, they should be bluer objects rather than ellipticals; otherwise, such models would overpredict the number counts for ellipticals. But if the additional population were blue objects, even though they would not make the predicted color distribution even worse, the predictions can not be ameliorated beyond $B - K = 5.5$ in the color distribution, and especially, the red-end humps beyond $B - K = 8.0$ can not be depressed. From the investigation of the color distribution, we arrive at the conclusion that there is no room for an additional galaxy population to be introduced into the models without first revising the traditional formation and evolution scenario for ellipticals.

We have considered a simple number-evolution model phenomenologically to show that number evolution could be the right answer to the question regarding the formation and evolution of elliptical galaxies. In particular, if the cosmic geometry is open or Λ -dominated, our work supports the idea that ellipticals formed by mergers of spiral galaxies, which is compatible with the prediction of hierarchical theory for formation and evolution of galaxies. In a forthcoming work, we will construct a unifying number-evolution model to explain the observations concerning the faint galaxies at high redshifts.

PH gratefully acknowledge Mrs. G. Kauffmann for her kindly help, and Mr. S. Charlot for providing us with their latest spectral synthesis models. We thank Mr. Jon Loveday for his careful reading of the manuscript, and for his constructive comments and suggestions to improve this paper. We also thank The State Key Laboratory of Science and Engineering Computing (LSEC) of Academia Sinica for providing us with computer supports. This work is in part supported by the National Natural Science Foundation of China.

REFERENCES

- Abraham, R. G., Tanvir, N. R., Santiago, B. X., Ellis, R. S., Glazebrook, K., & van den Bergh, S. 1996, MNRAS, 279, L47
- Babul, A., & Rees, M. J. 1992, MNRAS, 255, 346
- Babul, A., & Ferguson, H. C. 1996, ApJ, 458, 100
- Baugh, C. M., Cole, S., & Frenk, C. S. 1996, MNRAS, 282, L27
- Broadhurst, T. J., Ellis, R. S., & Shanks, T. 1988, MNRAS, 235, 827
- Broadhurst, T. J., Ellis, R. S., & Glazebrook, K. 1992, Nature, 355, 55
- Bruzual, A. G., & Kron, R. G. 1980, ApJ, 241, 25
- Bruzual, A. G., & Charlot, S. 1997, in preparation
- Carlberg, R. G., & Charlot, S. 1992, ApJ, 397, 5
- Cole, S. 1991, ApJ, 367, 45
- Cole, S., Aragon-Salamanca, A., Frenk, C. S., Navarro, J. F., & Zepf, S. E. 1994, MNRAS, 271, 781
- Colín, P., Schramm, D. N., & Peimbert, M. 1994, ApJ, 426, 459
- Colles, M., Ellis, R. S., Taylor, K., & Hook, R. N. 1990, MNRAS, 244, 408
- Colles, M., Ellis, R. S., Broadhurst, T. J., Taylor, K., & Bruce, A. 1993, MNRAS, 261, 19
- Cowie, L. L. 1991, Phys. Scripta, T36, 102
- Cowie, L. L., Songaila, A., & Hu, E. M. 1991, Nature, 354, 460
- Cowie, L. L., Songaila, A., Hu, E. M., & Cohen, J. G. 1996, AJ, 112, 839
- Djorgovski, S., Soifer, B. T., Pahre, M. A., Larkin, J. E., Smith, J. D., Neugebauer, G. et al. 1995, ApJ, 438, L13
- Driver, S. P., Phillipps, S., Davies, J. I., Morgan, I., & Disney, M. J. 1994, MNRAS, 266, 155
- Driver, S. P., Windhorst, R. A. 1995, preprint astro-ph/9511134
- Driver, S. P., Windhorst, R. A., Ostrander, E. J., Keel, W. C., Griffiths, R. E., & Ratnatunga, K. U. 1995, ApJ, 449, L23
- Driver, S. P., Windhorst, R. A., Phillipps, S., & Bristow, P. D. 1996, ApJ, 461, 525
- Efstathiou, G., Ellis, R. S., Peterson, B. A. 1988, MNRAS, 232, 431
- Eggen, O. J., Lynden-Bell, D., & Sandage, A. R. 1962, ApJ, 136, 748
- Ellis, R. S. 1997, ARA&A, 35, 389
- Fritze-v.Alvensleben, U., & Gerhard, O. E. 1994, A&A, 285, 751
- Fukugita, M., Takahara, F., Yamashita, K., & Yoshii, Y. 1990, ApJ, 361, L1
- Fukugita, M., Shimasaku, K., Ikhikawa, T. 1995, PASP, 107, 945
- Gardner, J., Cowie, L. L., & Wainscoat, R. 1993, ApJ, 415, L9

- Gardner, J. P., Sharples, R. M., Frenk, C. S., Carrasco, B. E. 1997, *ApJ*, 480, L99
- Gardner, J. 1998, *PASP*, 110, 291
- Glazebrook, K., Peacock, J. A., Collins, C. A., & Miller, L. 1994, *MNRAS*, 266, 65
- Glazebrook, K., Ellis, R. S., Santiago, B. X., & Griffiths, R. 1995a, *MNRAS*, 275, L19
- Glazebrook, K., Peacock, J. A., Miller, J. A., Collins, C.A. 1995b, *MNRAS*, 275, 169
- Glazebrook, K. 1997, preprint astro-ph/9707333
- Gronwall, C., & Koo, D. C. 1995, *ApJ*, 440, L1
- Guiderdoni, B., & Rocca-Volmerange, B. 1990, *A&A*, 227, 362
- Guiderdoni, B., & Rocca-Volmerange, B. 1991, *A&A*, 252, 435
- He, P., & Zhang, Y. Z. 1998a, *MNRAS*, 298, 483 (HZ98)
- He, P., & Zhang, Y. Z. 1998b, *Commun. Theor. Phys.* (Beijing China), accepted
- Jones, L. R., Fong, R., Shanks, T., Ellis, R. S., & Peterson, B. A. 1991, *MNRAS*, 249, 481
- Kauffmann, G., White, S. D. M., & Guiderdoni, B. 1993, *MNRAS*, 264, 201
- Kauffmann, G., Guiderdoni, B., & White, S. D. M. 1994, *MNRAS*, 267, 981
- Kauffmann, G., Charlot, S., & White, S. D. M. 1996, *MNRAS*, 283, L117
- Koo, D. C. 1981, PhD thesis, Univ. of California, Berkeley
- Koo, D. C. 1985, *AJ*, 90, 418
- Koo, D. C., & Kron, R. G. 1992, *ARA&A*, 30, 613
- Lacey, C. G., Guiderdoni, B., Rocca-Volmerange, B., & Silk, J. 1993, *ApJ*, 402, 15
- Lidman, C. E., & Peterson, B. A. 1996, *MNRAS*, 279, 1357
- Lilly, S. J., Cowie, L. L., & Gardner, J. P. 1991, *ApJ*, 369, 79
- Loveday, J., Peterson, B. A., Efstathiou, G., Maddox, S. J. 1992, *ApJ*, 390, 338
- Maddox, S. J., Sutherland, W. J., Efstathiou, G., Loveday, J., & Peterson, B. A. 1990, *MNRAS*, 247, 1p
- Marzke, R. O., Geller, M. J., Huchra, J. P., Corwin Jr., H. G. 1994, *AJ*, 108, 437
- McLeod, B.A., Bernstein, G. M., Rieke, M. J., Tollestrup, E. V., & Fazio G. G. 1995, *ApJS*, 96, 117
- Metcalf, N., Shanks, T., Fong, R., & Jones, L. R. 1991, *MNRAS*, 249, 498
- Metcalf, N., Shanks, T., Fong, R., & Roche, N. 1995, *MNRAS*, 273, 257
- Metcalf, N., Shanks, T., Campos, A., Fong, R., Gardner, J. P. 1996, *Nature*, 383, 236
- Mobasher, B., Ellis, R. S., & Sharples, R. M. 1986, *MNRAS*, 223, 11
- Moustakas, L. A., Davis, M., Graham, J. R., Silk, J., Peterson, B. A., & Yoshii, Y. 1997, *ApJ*, 475, 445
- Partridge, R. B., & Peebles, P. J. E. 1967, *ApJ*, 147, 868
- Pozzetti, L., Bruzual A., G., & Zamorani, G. 1996, *MNRAS*, 281, 953
- Rocca-Volmerange, B., & Guiderdoni, B. 1990, *MNRAS*, 247, 166
- Roukema, B. F., Peterson, B. A., Quinn, P. J., & Rocca-Volmerange, B. 1997, *MNRAS*, 292, 835
- Salpeter, E. E. 1955, *ApJ*, 121, 161
- Schechter, P. 1976, *ApJ*, 203, 297
- Scalo, J. M. 1986, *Fund. Cosmic Phys.*, 11, 1
- Shanks, T. 1989, *The Extra-Galactic Background Light*, ed. S. C. Bowyer & C. Leinert (Kluwer Academic Publishers), p.269
- Soifer, B. T., Matthews, K., Djorgovski, S., Larkin, J., Graham, J. R., Harrison, W., Jernigan, G., Lin, S. et al. 1994, *ApJ*, 420, L1
- Stevenson, P. R. F., Shanks, T., & Fong, R. 1986, *Spectral Evolution of Galaxies.*, ed. C. Chiosi & A. Renzini (Reidel, Dordrecht), p.439
- Szokoly, G. P., Subbarau, M. U., Connolly, A. J., Mobasher, B. 1998, *ApJ*, 492, 452
- Tinsley, B. M. 1980, *ApJ*, 241, 41
- Tyson, J. A. 1988, *AJ*, 96, 1
- Wang, B. 1991, *ApJ*, 383, L37
- White, S. D. M., & Frenk, C. S. 1991, *ApJ*, 379, 52
- Yoshii, Y. & Peterson, B. A. 1995, *ApJ*, 444, 15
- Yoshii, Y., & Takahara, F. 1988, *ApJ*, 326, 1
- Zepf, S. E. 1997, *Nature*, 390, 377

Zucca, E., Zamorani, G., Vettolani, G., Cappi, A., Merighi,
R., Mignoli, M., Stirpe, G. M., MacGillivray, H. et al.
1997, A&A, 326, 477

TABLE 1
OBSERVED COLORS OF GALAXIES

Type	$U - B^a$	$B - V^a$	$B - R^b$	$b_j - I^c$	$b_j - K^b$
E/S0	0.43	0.95	1.83	2.39	4.16
Sab	0.19	0.79	1.65	2.15	3.88
Sbc	0.07	0.68	1.30	1.78	3.64
Scd	-0.04	0.60	1.16	1.56	3.23
Sdm	-0.17	0.47	1.05	1.27	2.80

^aMixed from Fukugita et al. (1995);

^bMixed from Yoshii et al. (1988);

^cMixed from Yoshii et al. (1988, modelled) and Lidman et al. (1996).

TABLE 2
EXTINCTION MAGNITUDES FOR B , I , AND K BANDS AT DIFFERENT REDSHIFTS

z	B		I		K	
	E/S0 ^a	Others ^a	E/S0 ^a	Others ^a	E/S0 ^a	Others ^a
0	0.05	0.10	0.02	0.03	0.002	0.005
1	0.20	0.36	0.07	0.13	0.01	0.02
2	0.42	0.64	0.15	0.27	0.02	0.04
3	0.65	0.83	0.25	0.44	0.04	0.07
4	0.86	0.92	0.37	0.60	0.06	0.11
5	1.02	0.97	0.50	0.73	0.08	0.15

^aThe optical depth $\tau_0^*=0.10$, geometrical parameter $\zeta=0.50$ for ellipticals; $\tau_0^*=0.20$, $\zeta=0.25$ for the other types.

TABLE 3
MODEL PARAMETERS AND PREDICTED COLORS

Scenario A									
Type	τ_e^a	$U - B$	$B - V$	$B - R$	$b_j - I$	$b_j - K$	α^b	ϕ^{*b}	M_B^{*b}
E/S0	0.2	0.65	0.92	1.69	2.30	4.15	-0.70	9.68	-21.00
Sab	2.3	0.46	0.83	1.55	2.15	3.89	-1.25	3.85	-20.80
Sbc	4.6	0.11	0.61	1.24	1.81	3.45	-1.40	6.25	-20.80
Scd	9.5	-0.05	0.49	1.04	1.57	3.14	-1.45	5.75	-20.80
Sdm	∞	-0.15	0.39	0.88	1.37	2.87	-1.50	2.85	-20.70

Scenario B									
Type	τ_e^a	$U - B$	$B - V$	$B - R$	$b_j - I$	$b_j - K$	α^b	ϕ^{*b}	M_B^{*b}
E/S0	0	0.71	0.95	1.74	2.36	4.25	-0.70	9.68	-21.00
Sab	3.3	0.43	0.82	1.55	2.17	3.93	-0.95	4.05	-20.80
Sbc	6.3	0.11	0.62	1.26	1.84	3.51	-1.10	6.05	-20.80
Scd	13.5	-0.04	0.49	1.06	1.60	3.19	-1.50	5.75	-20.80
Sdm	∞	-0.13	0.41	0.92	1.42	2.95	-1.60	2.85	-20.70

Scenario C									
Type	τ_e^a	$U - B$	$B - V$	$B - R$	$b_j - I$	$b_j - K$	α^b	$\phi^{*[b,c]}$	$M_B^{*[b,c]}$
E/S0	0.05	0.72	0.95	1.74	2.37	4.26	-0.70	9.68	-21.00
Sab	3.5	0.40	0.81	1.54	2.15	3.91	-0.95	3.85	-20.80
Sbc	7.0	0.08	0.60	1.23	1.81	3.47	-1.05	6.25	-20.80
Scd	15.0	-0.05	0.49	1.06	1.59	3.18	-1.45	5.75	-20.80
Sdm	∞	-0.13	0.41	0.92	1.43	2.96	-1.55	2.85	-20.70

^a τ_e is the timescale of SFR, measured in Gyr;

^b α , ϕ^* , and M_B^* are parameters for LFs, ϕ^* in units of 10^{-4}Mpc^{-3} ;

^cThe Hubble constant has been scaled to $h = 0.5$ for Scenario C.

TABLE 4
PARAMETERS OF MERGER MODEL.

Model parameter	Scenario A	Scenario B	Scenario C
z_t	5.0	1.0	1.0
Q_{n1}	0.05	0.05	0.1
Q_{n2}	...	2.0	2.0
Q_m	0.3	0.2	0.1

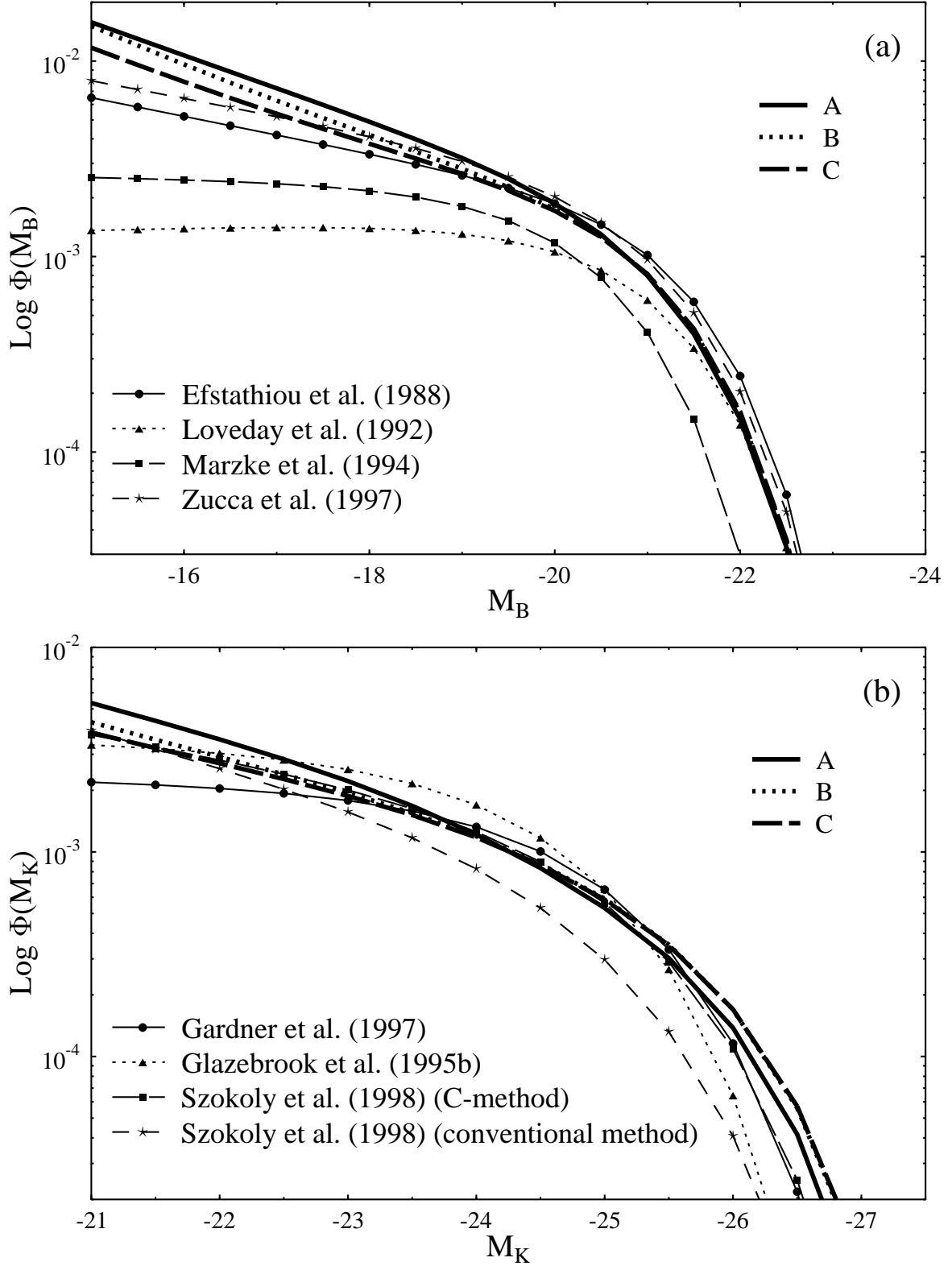


Fig. 1.— The present-day luminosity functions of galaxies. The models are indicated by thick lines, whose values are corresponding to those in Table 3, and the capital letters A, B, and C refer to Scenario A, B, and C respectively. The observational data are shown by thin lines decorated with various markers, and the sources of these observations are also indicated in the figure. Notice that the characteristic density ϕ^* and mixing ratio between different galaxies of Efstathiou et al. (1988) LF are taken from Pozzetti et al. (1996). Panels (a) and (b) are for B - and K -bands respectively. The Hubble constant has been scaled to $h = 0.5$ for Scenario C.

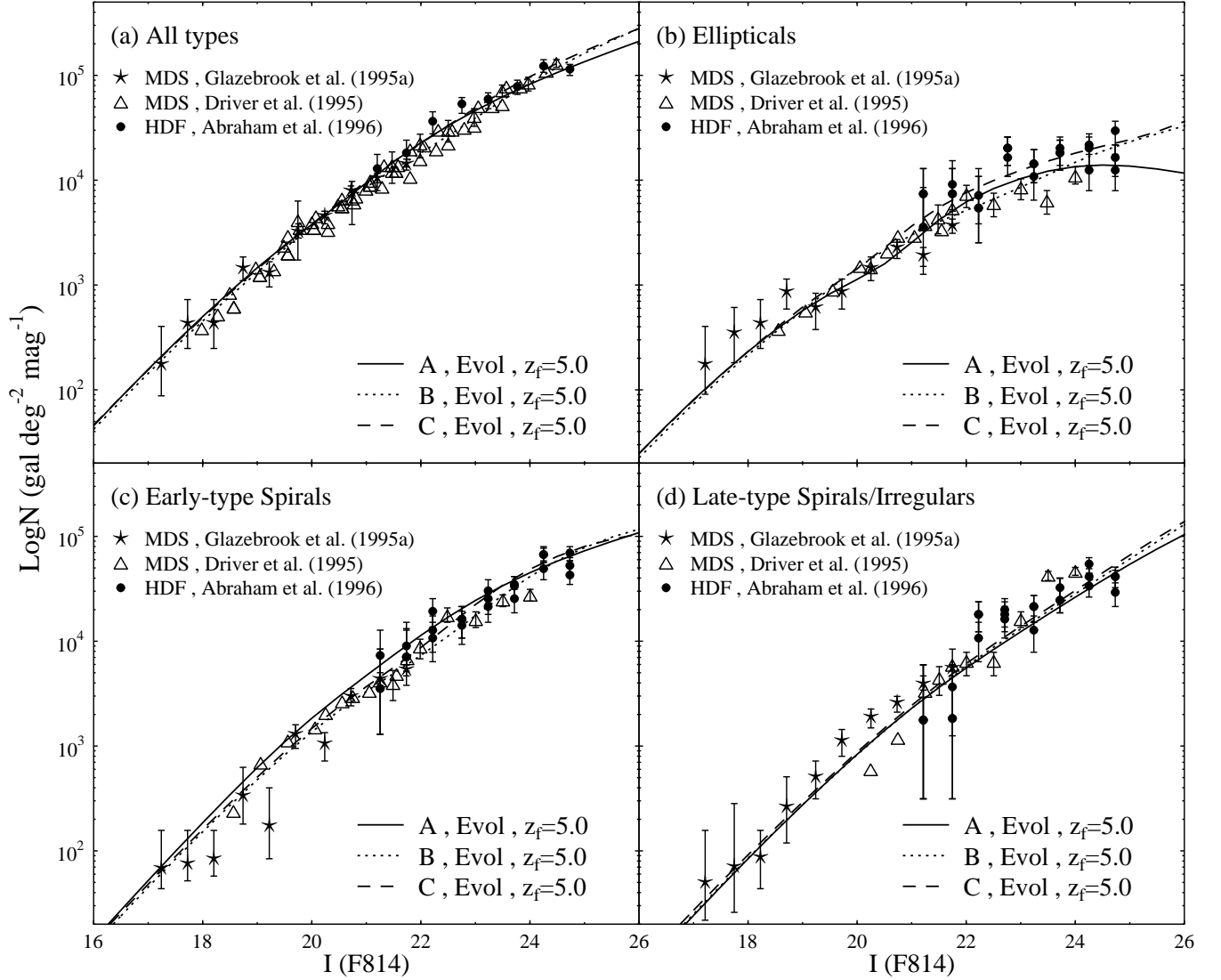
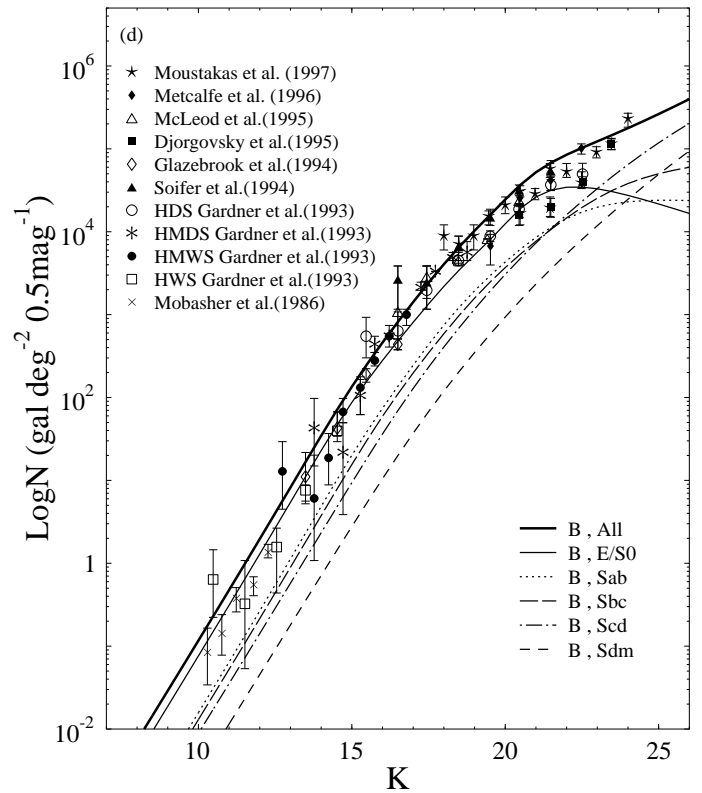
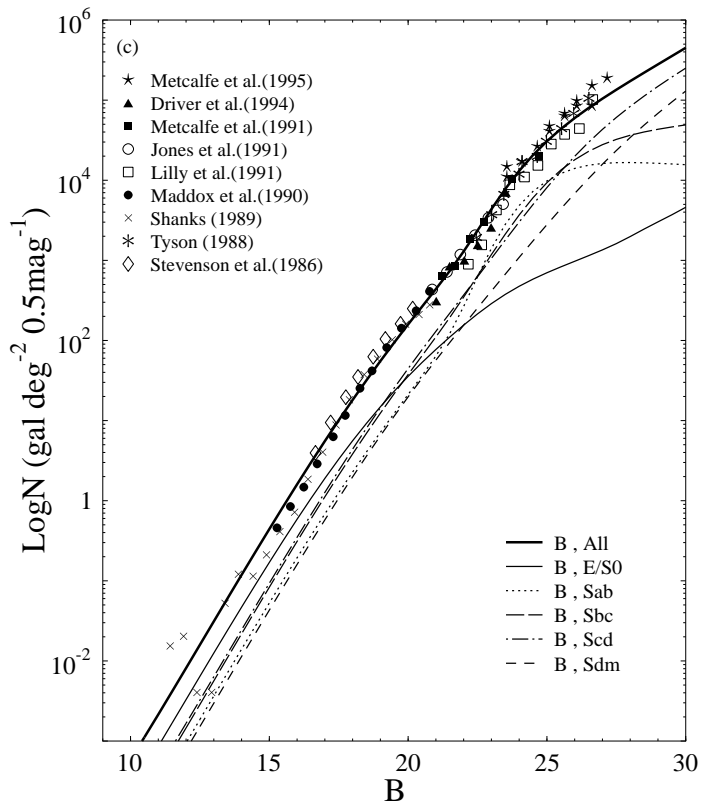
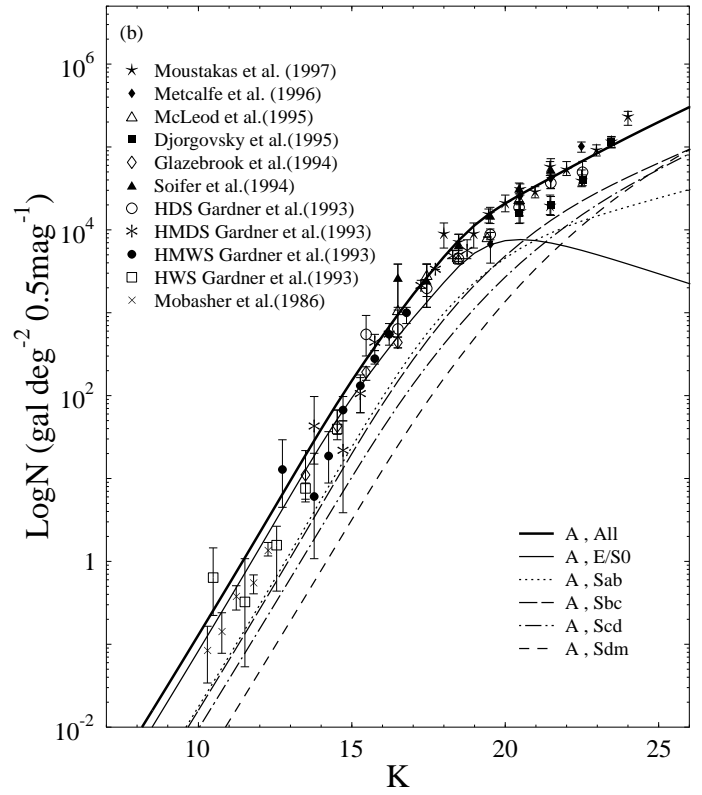
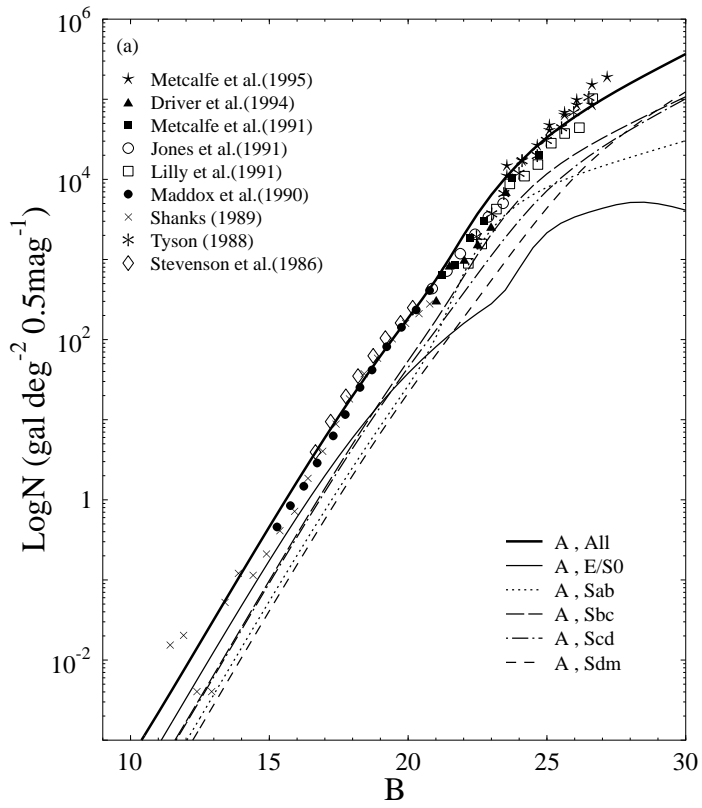


Fig. 2.— Differential number counts as a function of apparent magnitude in I_{814} -band. The sources of observational data are exhibited in the figure and these data are indicated by symbols. Predictions of models are shown by lines. Panels (b), (c), and (d) are for ellipticals, early-type spirals, and late-type spirals/irregulars respectively, and (a) for the overall population. Here and hereafter, capital letters A, B, and C represent Scenario A, B, and C, respectively.



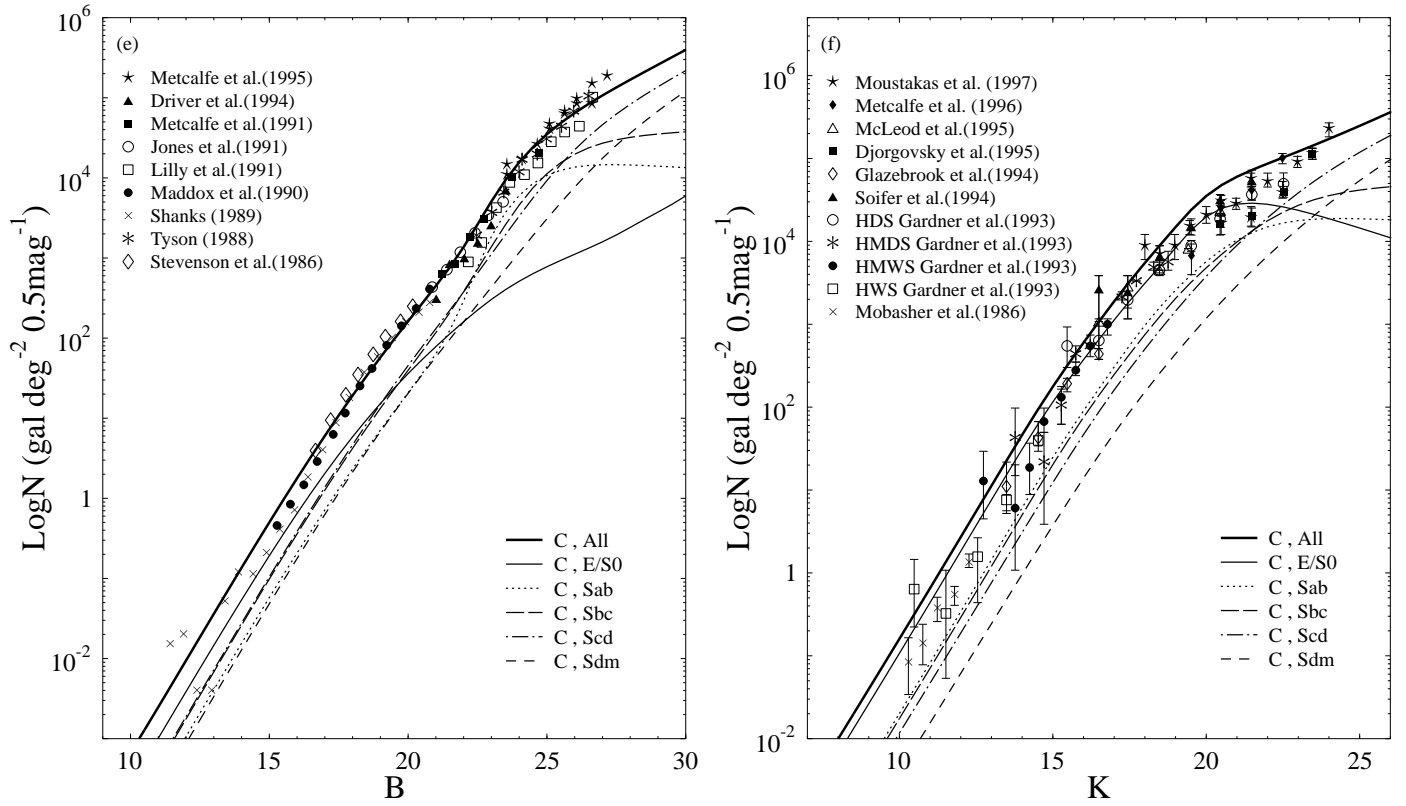


Fig. 3.— Differential number counts as a function of apparent magnitude in B - (panel a, c, and e) and K - (panel b, d, and f) bands. Panels (a) and (b) are for Scenario A, (c) and (d) for Scenario B, and (e) and (f) for Scenario C, respectively. The sources of observational data are exhibited in the figure. Predictions of models are shown by lines.

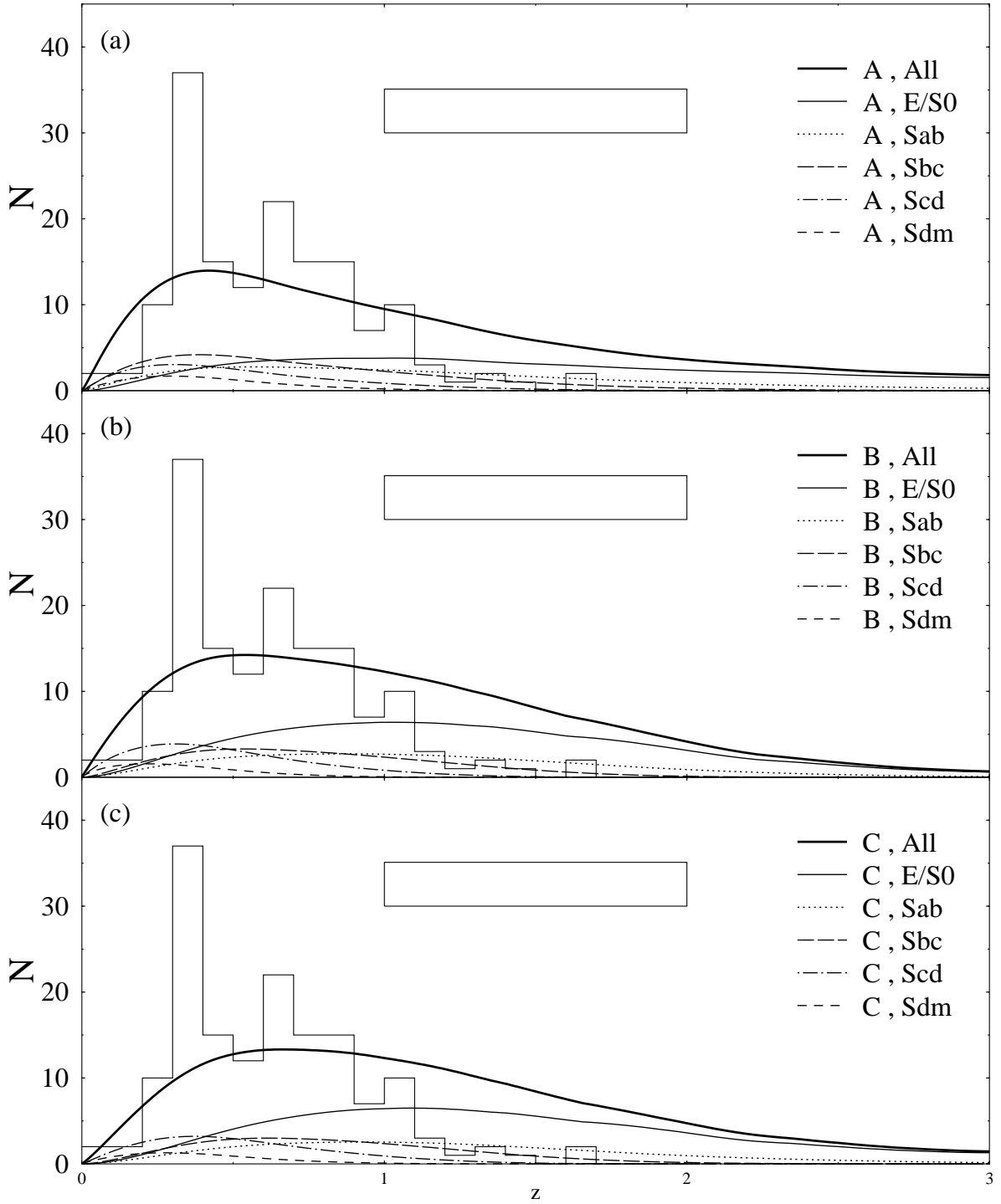


Fig. 4.— Redshift distribution for galaxies limited to $K < 20$. The observational data are derived from Cowie et al. (1996), and are shown by the solid histograms. Predictions of models are shown by lines. The model predictions have been normalized to the total number of both z -identified and z -unidentified objects ($N_{id} + N_{no-id}$). The area of the rectangle in each panel equals the number of unidentified objects (N_{no-id}). Panels (a), (b), and (c) are for Scenario A, B, and C respectively.

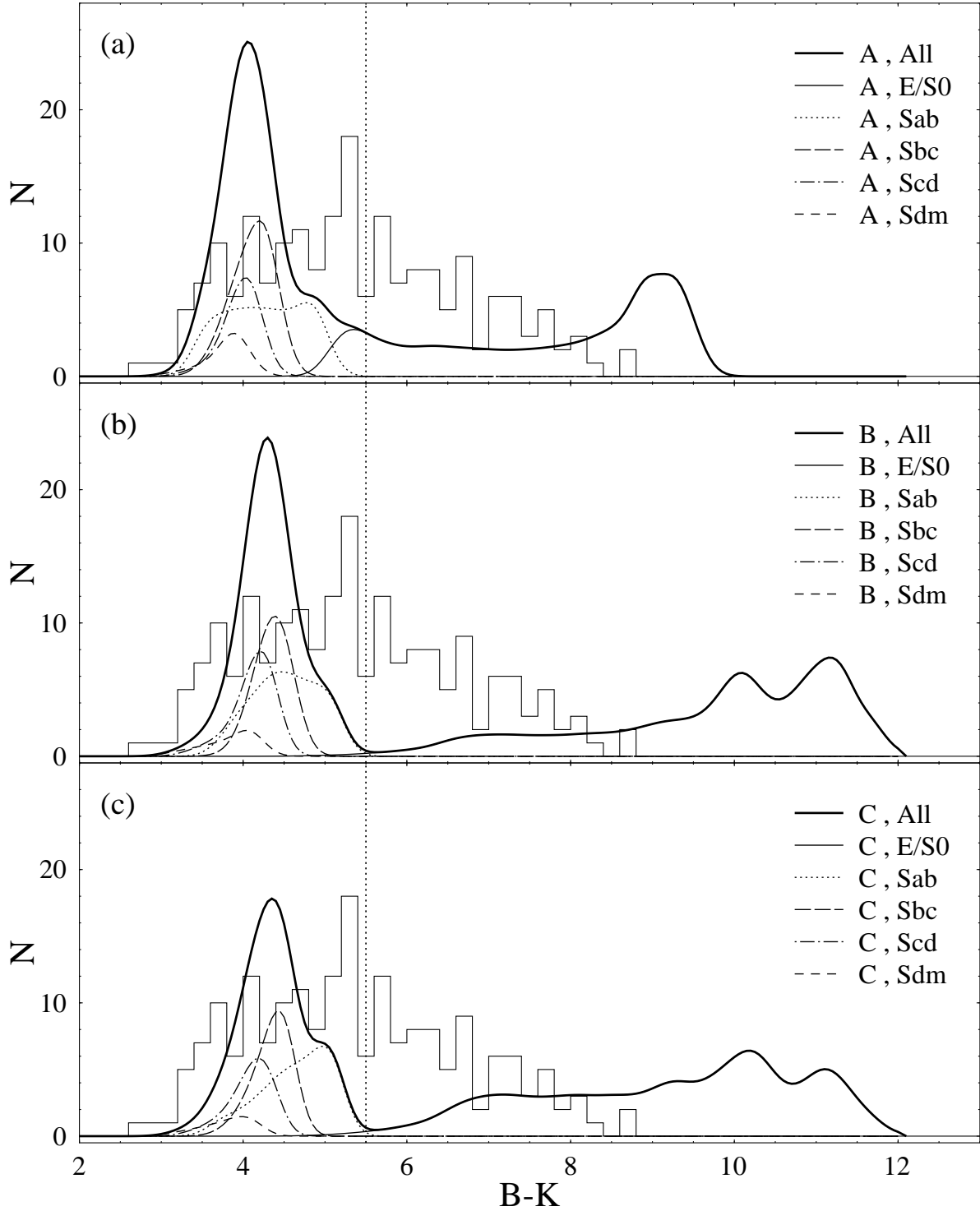


Fig. 5.— $B - K$ color distribution for $17 < K < 20$. The solid histogram shows the observed distribution derived from Cowie et al. (1996). The predictions are shown by various lines. Panels (a), (b), and (c) are for Scenario A, B, and C, respectively. To aid the eye, we draw a vertical dotted line at $B - K = 5.5$ for the reason explained in the text. The model predictions have been normalized to the total number of objects enclosed by the histogram.

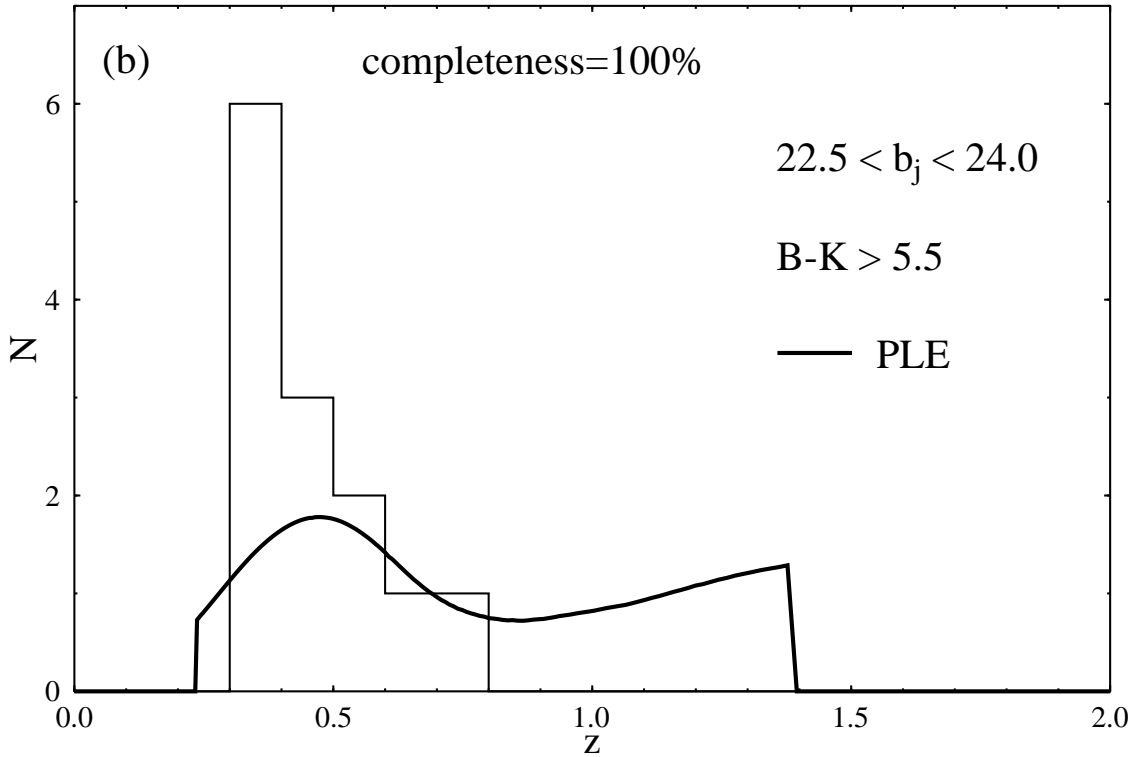
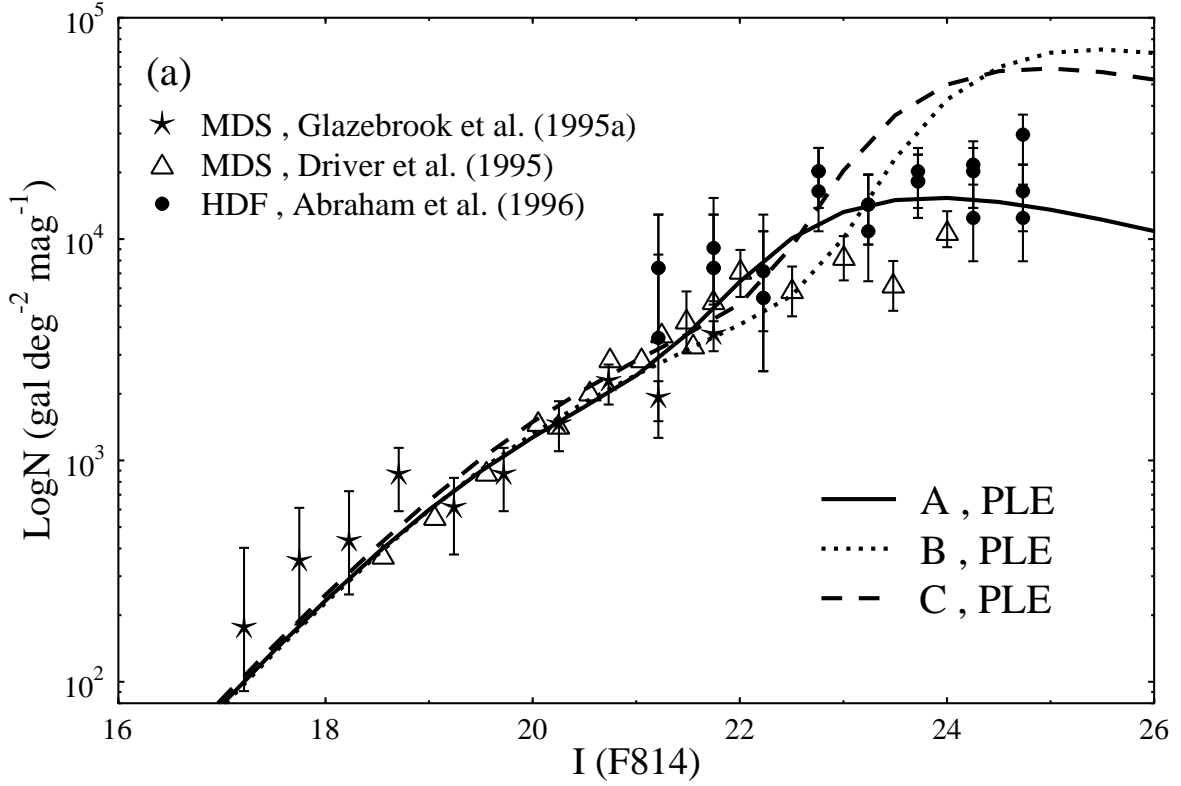


Fig. 6.— (a) Differential number counts as a function of apparent magnitude in I_{814} -band. The sources of observational data are exhibited in the figure and these data are indicated by symbols. Predictions of pure luminosity evolution (PLE) models are shown by lines. (b) Redshift distribution for galaxies limited to $22.5 < b_j < 24.0$ and with the constraint of $B - K > 5.5$. The observational data are derived from Cowie et al. (1996), which are shown by the solid histogram. The model prediction is shown by the solid line, and it has been normalized to the total number of the objects enclosed by the histogram.

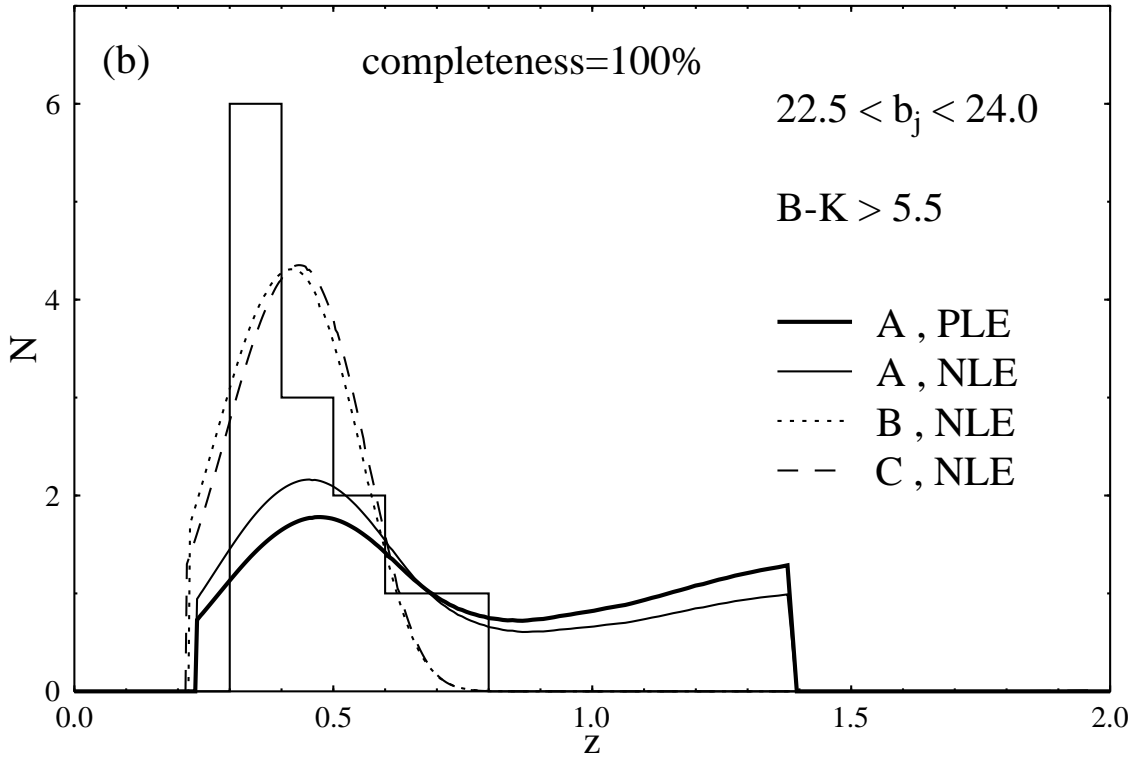
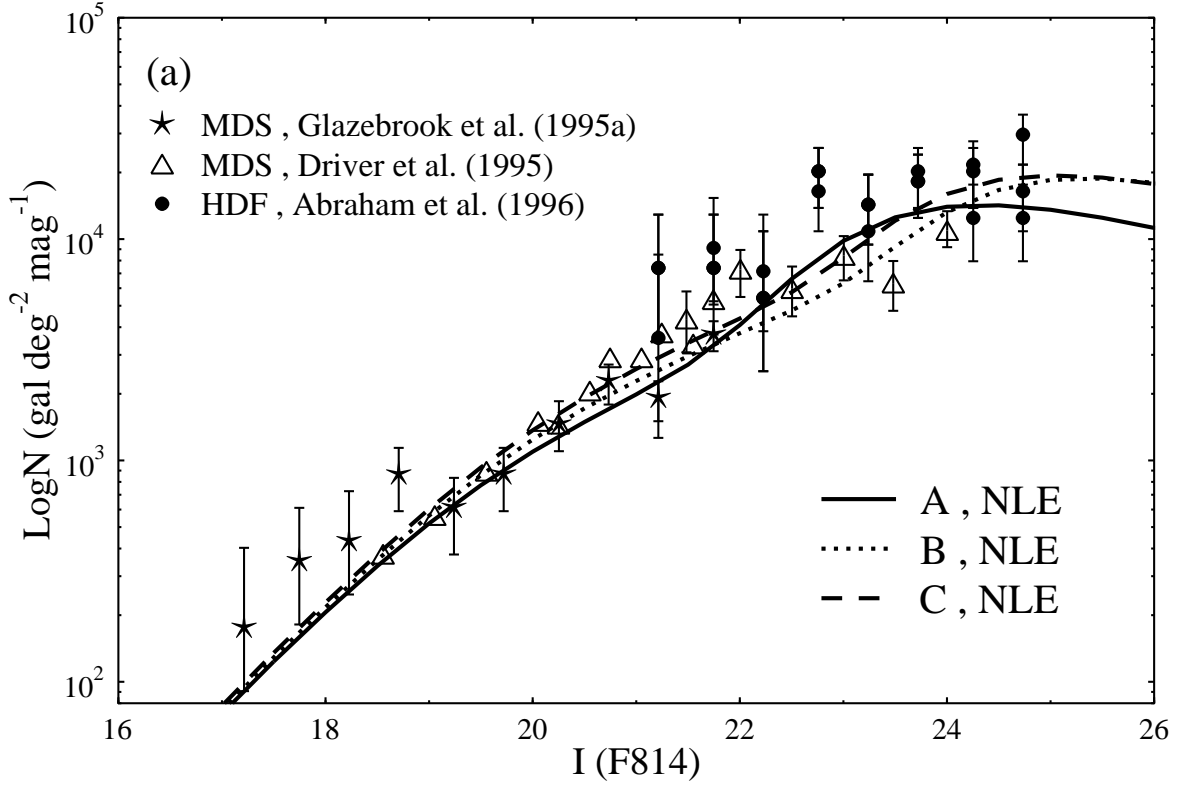


Fig. 7.— (a) Differential number counts as a function of apparent magnitude in I_{814} -band. Predictions of number-luminosity evolution (NLE) models are shown by lines. (b) Redshift distribution for galaxies limited to $22.5 < b_j < 24.0$ and with the constraint of $B - K > 5.5$. The model predictions are shown by lines, and they have been normalized to the total number of the objects enclosed by the histogram.

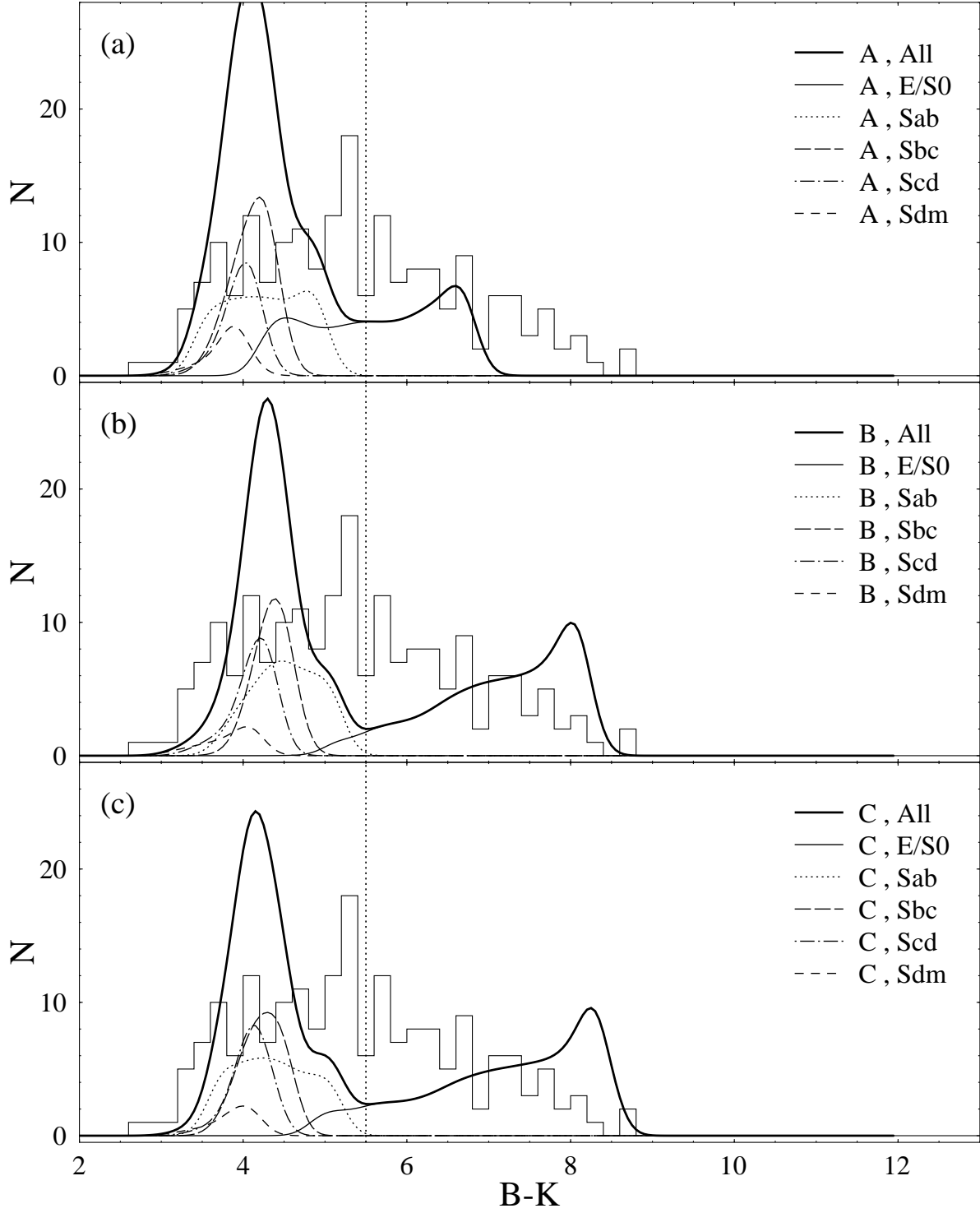


Fig. 8.— The same as Figure 5, but the predictions are made by the NLE assumption for ellipticals, described by Eq. [2] and [3].